DC Ripple Component Cancelation Method of Isolated AC-DC Converter with Matrix Converter for Input Current Harmonics Reduction

Shunsuke Takuma
Dept. of Electrical, Electronics, and Information Engineering
Nagaoka University of Technology
Nagaoka, Japan
takuma_s@stn.nagaokaut.ac.jp

Keisuke Kusaka
Dept. of Electrical, Electronics, and Information Engineering
Nagaoka University of Technology
Nagaoka, Japan
kusaka@vos.nagaokaut.ac.jp

Jun-ichi Itoh
Dept. of Electrical, Electronics, and Information Engineering
Nagaoka University of Technology
Nagaoka, Japan
itoh@vos.nagaokaut.ac.jp

***Abstract*— This paper proposes a current ripple cancelation method in DC side for an isolated AC-DC converter with a matrix converter. In this system, input currents are distorted by an error between a reference and actual input current caused by a ripple component at a dc current in the output side when the smoothing inductor in the output side is minimized. The proposed ripple cancellation method combines current slopes during positive with negative cycles of a high-frequency current. In addition, dead-time-induced voltage error is also reduced by the extension of a minimum pulse width of each switch in the matrix converter with the proposed method. It is demonstrated that the input current total harmonic distortion (THD) is improved by eliminating the ripple components regardless of the amplitude of the ripple component. From the experimental results with the 10-kW prototype, the input current THD is reduced from 8.2% to 5.3% at the 0.2 p.u..**

Keywords—matrix converter, space vector control, three-phase AC to DC converter, current ripple cancellation

I. INTRODUCTION

Recently, electric vehicles and hybrid vehicles have been actively developed to reduce an environmental load substance such as CO_2. A rapid charger is required to improve usability for consumers. A battery charger with a low power system is used as a DC-DC converter without the galvanic isolation or a single-phase AC to DC converter [1]-[3]. Generally, a rapid charger with a large power capacity consists of a three-phase PWM rectifier and an isolated DC-DC converter. However, three boost inductors at the grid side and the DC-link capacitor are required [4]-[6]. Therefore, an isolated AC-DC converter with a buck-type matrix converter has been researched to reduce such passive components [7]-[14]. Both the DC link capacitor and boost inductors are removed by the direct conversion from grid-frequency AC to high-frequency AC with a matrix converter.

The current ripple of a dc current in the output side becomes large when the inductance of a smoothing inductor decreases to achieve the high-power density. The iron loss and switching loss increases due to the high switching frequency to reduce the volume of the smoothing inductor. However, the input current also is conposed by an output current ripple due to the use of a minimized smoothing inductor in the dc side because the output current is assumed to be constant in the conventional control methods in order to simplify the control strategy. Furthermore, the volume of the input filter also becomes large to achieve the low input current distortion because low-order harmonics of the output current ripple affects the input currents.

In order to solve this problem, the optimized switching pattern has been proposed to achieve the minimum current ripple at the dc side [13]. However, the input currents still distort by the incomplete cancelation of the current ripple. In addition, the input current ripple is increased compared with that of the conventional control scheme. In [14], the improvement of the eight-segment control method has been proposed to cancel the control error due to the current ripple. However, this duty calculation requires the smoothing inductor value. Therefore, the input currents may still distort by the error between the actual inductor value and nominal inductor value. In addition, the output voltage is not linearized by the dead-time for the commutation of the matrix converter in the low modulation index. The authors confirmed the verification by simulation results only.

In this paper, the cancelation of the output current ripple is proposed in order to reduce the harmonics components in the input current. The original idea of this paper is that the cancelation of the output current ripple is independent of the smoothing inductor value and linearization of the relationship between the reference and actual voltage. The effect of the output current ripple is eliminated by changing the switching pattern. The fundamental operation is obtained by the experiment with a 10 kW proto-type. The input current distortion is reduced by the proposed method regardless of the output current ripple.

II. PROPOSED DC CURRENT RIPPLE CANCELATION METHOD

Figure 1 shows the circuit configuration of the isolated AC-DC converter with the buck-type matrix converter. The input currents and output DC voltage are controlled by the buck-type matrix converter with the space vector control (SVM). The smoothing capacitor and initial charger circuit are not required by applying the matrix converter at the primary side of the transformer.

Figure 2 shows the control diagram using traditional SVM. The traditional SVM is based on the constant output current during one switching periods. V_z is defined as zero vectors V_7, V_8, and V_9. The output voltage vectors V_1, V_2, and V_z are selected during the first half switching periods to generate a positive voltage. On the other hands, the output voltage vectors V_4, V_5, and V_z are selected during the other half periods to generate the negative voltage. These duty reference T_1, T_2, and T_z are calculated by

$$T_1 = \frac{1}{|A|}\begin{vmatrix} v_\alpha & V_{2\alpha} \\ v_\beta & V_{2\beta} \end{vmatrix} \quad (1),$$

$$T_2 = \frac{1}{|A|}\begin{vmatrix} V_{1\alpha} & v_\alpha \\ V_{1\beta} & v_\beta \end{vmatrix} \quad (2),$$

$$T_z = 1-(T_1+T_2)\left(\because \begin{vmatrix} V_{1\alpha} & V_{2\alpha} \\ V_{1\beta} & V_{2\beta} \end{vmatrix}\right) \quad (3),$$

where v_α and v_β are αβ components of the input current reference, $v_{1\alpha}$, $v_{1\beta}$, $v_{2\alpha}$, and $v_{2\beta}$ are also αβ components of the vectors V_1 and V_2 which are selected based on the area located in the input current reference.

Figure 3(a) shows the operation waveforms of the voltage and current at the primary side of the transformer, the ideal dc current without the current ripple, and the input current. It is assumed that the transformer is the ideal condition without the leakage inductance and magnetic inductance. The conventional control method assuming the ideal dc current simply regulates the input current to the reference.

Figure 3(b) shows the operation waveforms of the voltage and current at the primary side of the transformer, the non-ideal dc current with the current ripple, and the input current when the conventional control method is applied. In this case, the actual input current at S-phase has the error which is the shaded area due to the DC current ripple. In particular, R-phase and S-phase current are lower and higher than the input current reference, respectively, leading to the distortion of the input current. The duty compensation for the error caused by the output current ripple is difficult because the relationship between the duty and the input current is nonlinear. Therefore, the cancellation method of the DC current ripple during one switching periods is proposed to suppress the input current distortion.

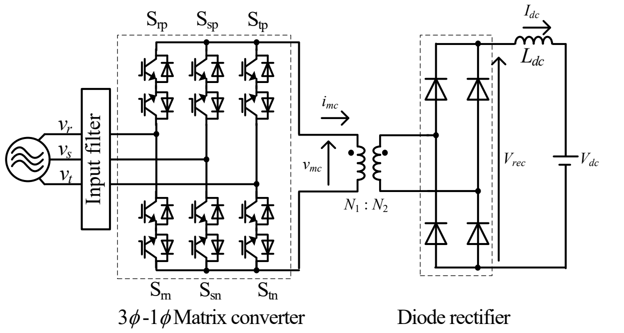

Fig. 1. Circuit configuration of isolated AC-DC converter using buck-type matrix converter. The isolated AC-DC converter consists of the three-phase to single phase matrix converter, the high-frequency transformer, the diode rectifier, and the smooting inductor.

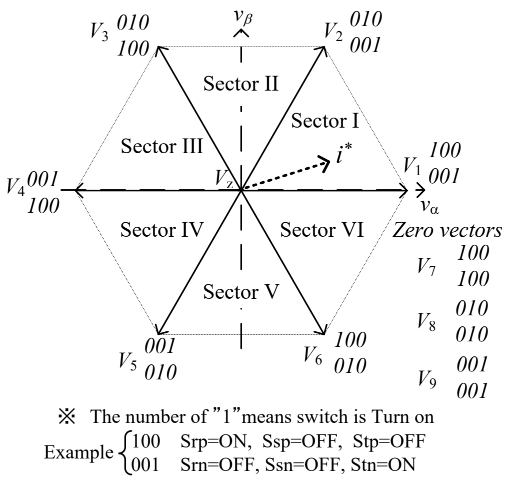

Fig. 2. Space vector control.

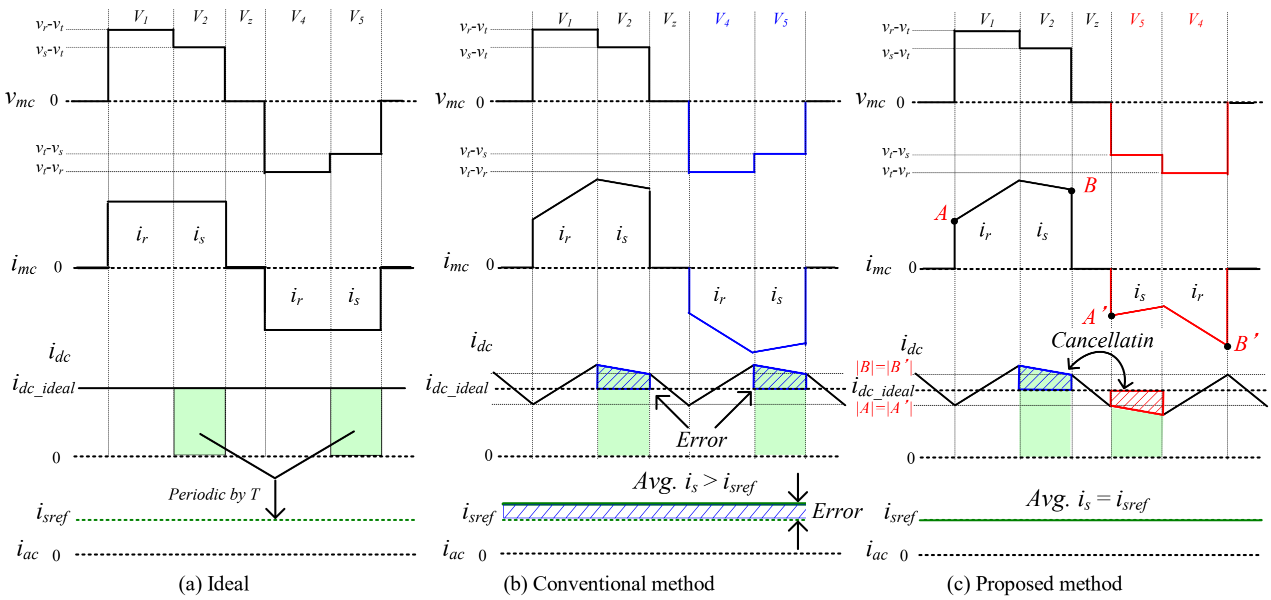

Fig. 3. Effect of dc current ripple against input current. The error between the reference and actual current of the input current is caused by the dc current ripple with the conventional control method. In the proposed control method, the ripple component of the phase-current during one switching periods is cancelled to by changing the order of the selected voltage vectors.

Figure 3(c) shows the operation waveforms of the voltage and current at the primary side of the transformer, the non-ideal dc current with the current ripple, and the input current when the proposed control method is applied. The effect of the dc current ripple is eliminated by changing the switching pattern during half cycle. The order of the output voltage vector V_4 and V_5 is alternated compared to the conventional control method. The advantages of the changing waveforms are as follow: 1) Cancellation of the ripple current 2) Extension of the pulse width. The detail of the two advantages is explained in the next chapter.

A. Principle of current ripple cancellation

Figure 4 depicts the ripple cancellation principle for the input current during one switching period. Two amplitudes at point A and B are equal to those at point A' and B', respectively. The solid line and dotted line depict the instantaneous currents from point A to B and A' to B' during the transition of the output vectors V_1, V_2 and V_4, V_5, respectively. The average currents I_{ave1}, I_{ave2} during durations T_1, T_2 are expressed as

$$I_{ave} = I_{ave1} = I_{ave2} = \frac{i_0 + i_2}{2} \tag{4}$$

where, i_0 is the initial current at V_1, and i_2 is the final state at V_2. Therefore, the input current is controlled by the proposed cancellation method regardless of the amplitude of the ripple components. Therefore, the duty for the proposed control method is calculated by Eq. (1)-(3) without the inductor parameter. By applying the proposed method, the periodic output current of the matrix converter is controlled to the constant current which is necessary to use the traditional SVM.

B. Analytical results of DC current ripple

In this chapter, the DC current ripple with the proposed method is clarified to design the inductor at the DC side.

Figure 5 shows the rectified voltage V_{rec}, DC voltage V_{dc}, and the instantaneous current of the inductor at the DC side during one switching cycle. The output voltage of the matrix converter is controlled to cancel the DC current ripple. The amplitudes of the current ripple $I_{p\text{-}p1}$ and $I_{p\text{-}p2}$ with the conventional and proposed method are expressed as

$$I_{p-p1} = \begin{cases} \dfrac{(Nv_1 - V_{dc})T_1}{L_{dc}} & \because \quad {}_{dc} > Nv_2 \\[2ex] \dfrac{(Nv_1 - V_{dc})T_1 + (Nv_2 - V_{dc})T_2}{L_{dc}} & \because \quad /v_2 > V_{dc} \end{cases} \tag{5}$$

$$I_{p-p2} = \begin{cases} \dfrac{(Nv_1 - V_{dc})T_1 - (Nv_2 - V_{dc})T_2}{L_{dc}} & \because \quad {}_{dc} > Nv_2 \\[2ex] \dfrac{(Nv_1 - V_{dc})T_1 + (Nv_2 - V_{dc})T_2}{L_{dc}} & \because \quad /v_2 > V_{dc} \end{cases} \tag{6}$$

where N is the turn ratio of the transformer, L_{dc} is the inductance of the inductor at the DC side, and v_1 and v_2 are the maximum and medium line to line voltage.

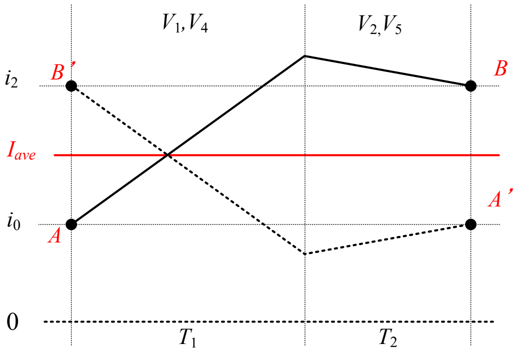

Fig. 4. Principle of current ripple cancellation.

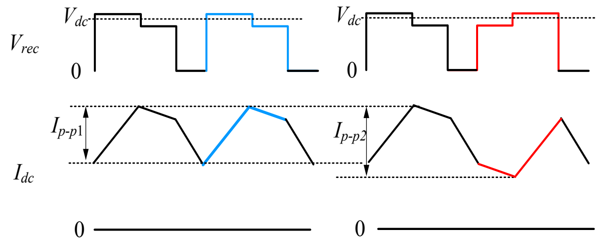

(a) $Nv_1 > V_{dc} > Nv_2$

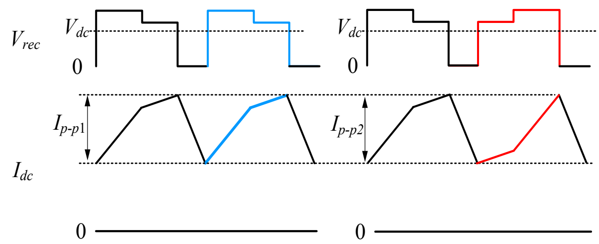

(b) $Nv_1 > Nv_2 > V_{dc}$

Fig. 5. DC current ripple waveforms. The DC current ripple is decided by the grid voltage, DC voltage, and turn ration of the transformer.

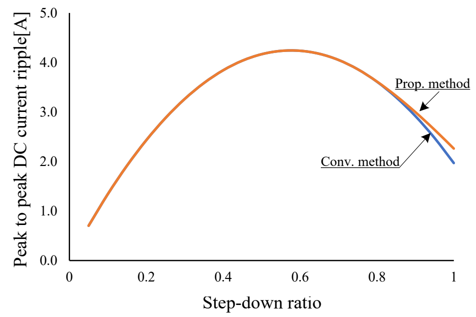

(a) Amplitude of ripple current

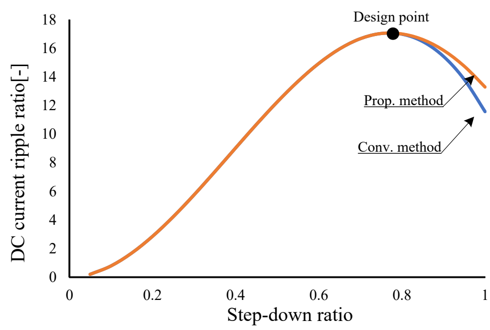

(b) Ripple current ratio

Fig. 6. Relationship between step-down ratio and DC current

Figure 6(a) shows the relationship between the step-down ratio and current ripple ratio. It is confirmed that the current ripple amplitude of the proposed method is larger than them of the conventional method over the 0.8 of the step-down ratio. However, the amplitude of the current ripple is the same under the 0.8 of the step-down ratio. The amplitude of the current ripple is depending on the relationship between the grid voltage, DC voltage, and turn ratio.

Figure 6(b) shows the relationship between the DC current ripple ratio and step-down ratio with the conventional and proposed method. It is assumed that the transition power is constant when the step-down ratio is changed by the matrix converter. Generally, the inductor at the DC side is designed by the requirement of the current ripple ratio. In a comparison of both the conventional and proposed topology design point, the step-down ratio is 0.77 because the worst current ripple ratio is the same. Therefore, the proposed method is not affected to design the inductor at the inductor.

C. *Limitation of proposed cancellation method*

The proposed cancellation method has the limitation to apply the matrix converter. The limitation is decided by the current ripple because the proposed method is based on a continuous current mode. If the matrix converter is operated by a discontinuous current mode under the voltage condition of Fig 5(a), the output current at the negative half cycle is zero because the DC voltage is larger than the output voltage of the matrix converter. However, the limitation to apply the proposed method is nothing when the DC voltage.

D. *Extension of minimum pulse width*

Figure 7(a) and 7(b) show the switching pattern during on switching period. It is assumed that two switches of the bi-directional switch turn-on and turn-off at the same time without the commutation. The relationship between each duration is $T_1 > T_2 > T_z$. The minimum pulse width is defined as the pulse width which is shorter than another pulse width in six bi-directional switches during one switching period. In the conventional method, the minimum pulse width is T_2 at the switches S_{sp} and S_{sn}. On the other hand, in the proposed method, the minimum pulse width is the width of the sum of T_2 and T_z at the switches S_{sp} and S_{sn}. Hence, the proposed method extends the minimum pulse width, leading to the reduction of the dead time effect.

Figure 8 shows the minimum duty in the conventional method and the proposed method. In the conventional method, the dead-time-induced output voltage error occurs when the minimum duty is lower than 5%. Therefore, the input current distortion becomes more severe due to the dead-time. Meanwhile, the minimum duty with the proposed method is always higher than that of the conventional method.

III. Experimental Verification

Table I shows the simulation and experimental conditions. The switching devices at the three-phase to single-phase matrix converter are IGBTs (MITSUBISHI ELECTRIC: CM400C1Y-24S). Note that the four-step voltage commutation [7] is applied to prevent the commutation failure such as the short-circuit of the grid voltage, whereas one step period of the four-step commutation is set to 1.0 μs. The inductor at the DC side is designed by the current ripple ratio which is lower than 10 % at the rated power.

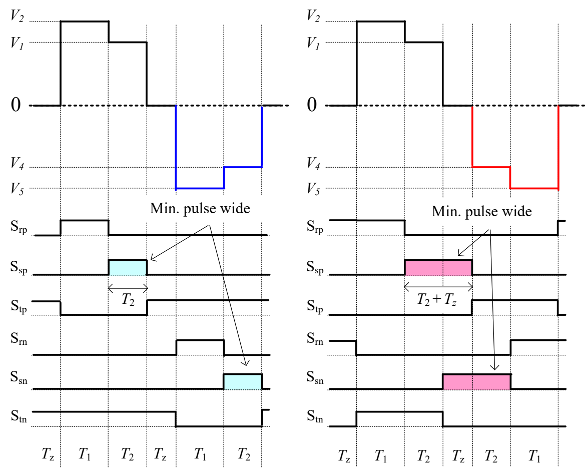

(a) Conventional method (b)Proposed method

Fig. 7. Comparison among minimum pulse width. The minimum pulse width is extended by the proposed method.

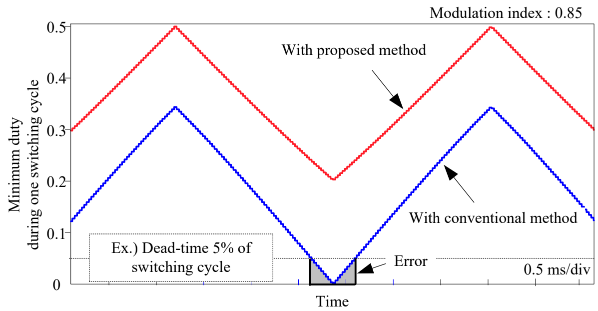

Fig.8. Minimum duty during one switching cycle.

TABLE I. Simulation and Experimental Conditions.

Element	Symbol	Value
Rated output power	P_{out}	10 kW
Grid voltage	v_{ac}	200 V
DC voltage	V_{dc}	400 V
DC inductor	L_{dc}	1.6 mH
Current ripple	$I_{p\text{-}p}$	2.5 A(10%※1)
Input filter	$L_f(\%Z)$	350 μH(2.3%)
	$C_f(\%Y)$	11 μF(4.7%)
Commutation time	T_d	1.0 μs
Carrier frequency	f_c	20 kHz
Turn ratio	N=N_2/N_1	2.4

※1 Current ripple is designed at rated output power.

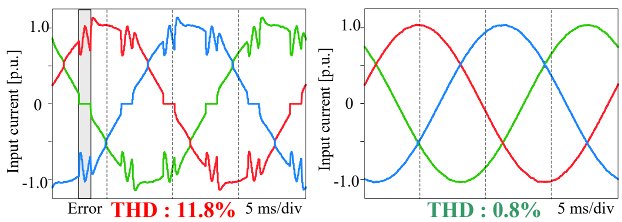

(a) Conventional method (b) Proposed method

Fig. 9. Comparison among minimum duty.

Figure 9(a) and (b) shows the input current waveforms and the harmonic analysis with the conventional and proposed control method. The same inductor value is used for the evaluation of each control method. The commutation operation and the input filter are not applied to evaluate only the effect of the dc current ripple. The input currents are distorted by the error caused by the dc current ripple with the conventional method, resulting in the high values of the 5th and 7th order harmonic components. In the proposed current ripple cancelation method, the input current THD is improved by 90% at a load of 0.2 p.u..

Figure 10(a) and (b) depicts the input current waveforms with dead-time of 5% against the switching cycle in the conventional method and the proposed method. In the conventional method, the minimum duty which is lower than dead-time is eliminated to avoid short-circuit. The input current distortion due to dead-time is dominant at the light load. Therefore, the input current THD is too large. On the other hands, the input current distortion is significantly reduced because the error due to the dead-time is suppressed by the proposed method.

Figure 11 shows the THD characteristics with the conventional and proposed control method when the dc the smoothing inductor is changed to adjust the DC current ripple. In the conventional method, the input current distortion due to the error is improved to decrease the ripple ratio of the dc current. However, the input current is still distorted due to DC current ripple because the output current is not constant such as an ideal current source. On the other hand, the input current THD is greatly improved by applying the proposed method regardless of the ripple ratio of the dc current. In other words, the error between the reference and actual current at the grid side is completely eliminated by the proposed method.

Figure 12(a) and (b) show the waveforms of the rectified voltage, DC voltage, and DC current with the conventional and proposed method at 0.2p.u.. The inductor is designed by the current ripple which is the maximum current ripple of 10%. The amplitudes of the current ripple with the conventional and proposed method are the same because the step-down ratio is 0.75.

Figure 13 (a) and (b) show the experimental waveforms with the conventional method at the high modulation index. Hence, the error between the reference and actual input current occurs due to the dc current ripple which is not eliminated in the conventional method. As a result, the input current THD is high at 4.1%. Meanwhile, Figure 13 (c) and (d) show the experimental waveforms with the proposed method at the high modulation index. Consequently, the input current THD is reduced from 4.1% to 3.3% at rated load compared to that of the conventional method.

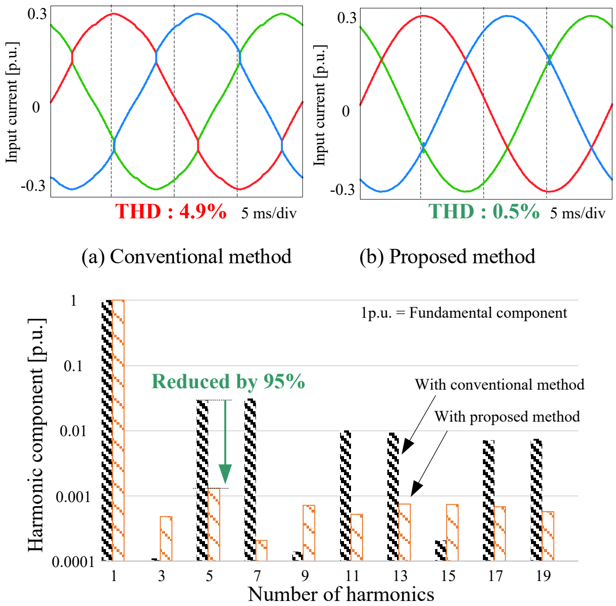

(a) Conventional method (b) Proposed method

(c) Harmonic analysis

Fig. 10. Harmonic comparison at load of 0.2p.u..

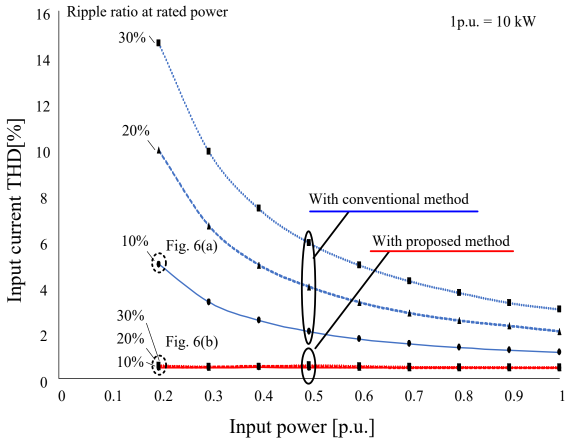

Fig. 11. Characteristic of input current THD against input power. The input current distortion due to the DC current ripple is suppressed by the proposed method every current ripple ratio.

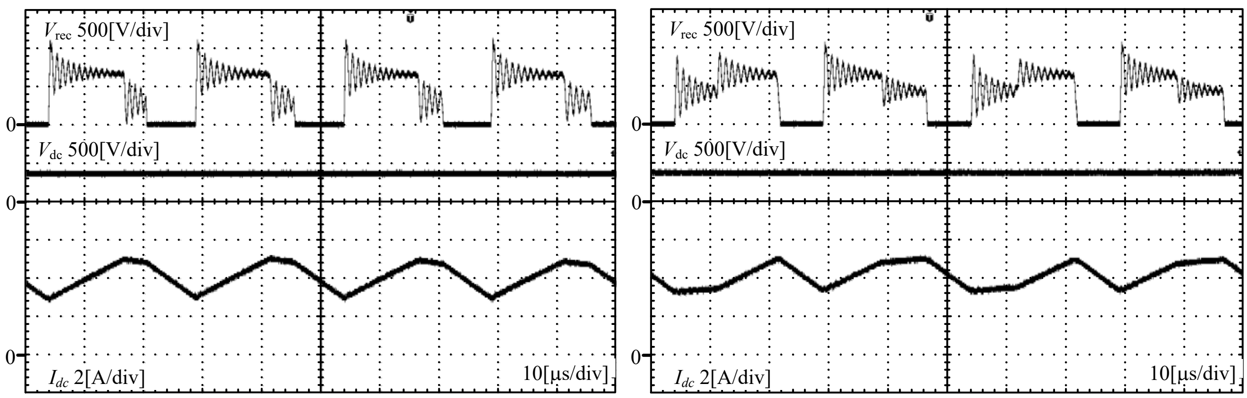

(a) Conventional method (b) Proposed method

Fig. 12. Voltage and current waveforms at DC side at 0.2p.u..

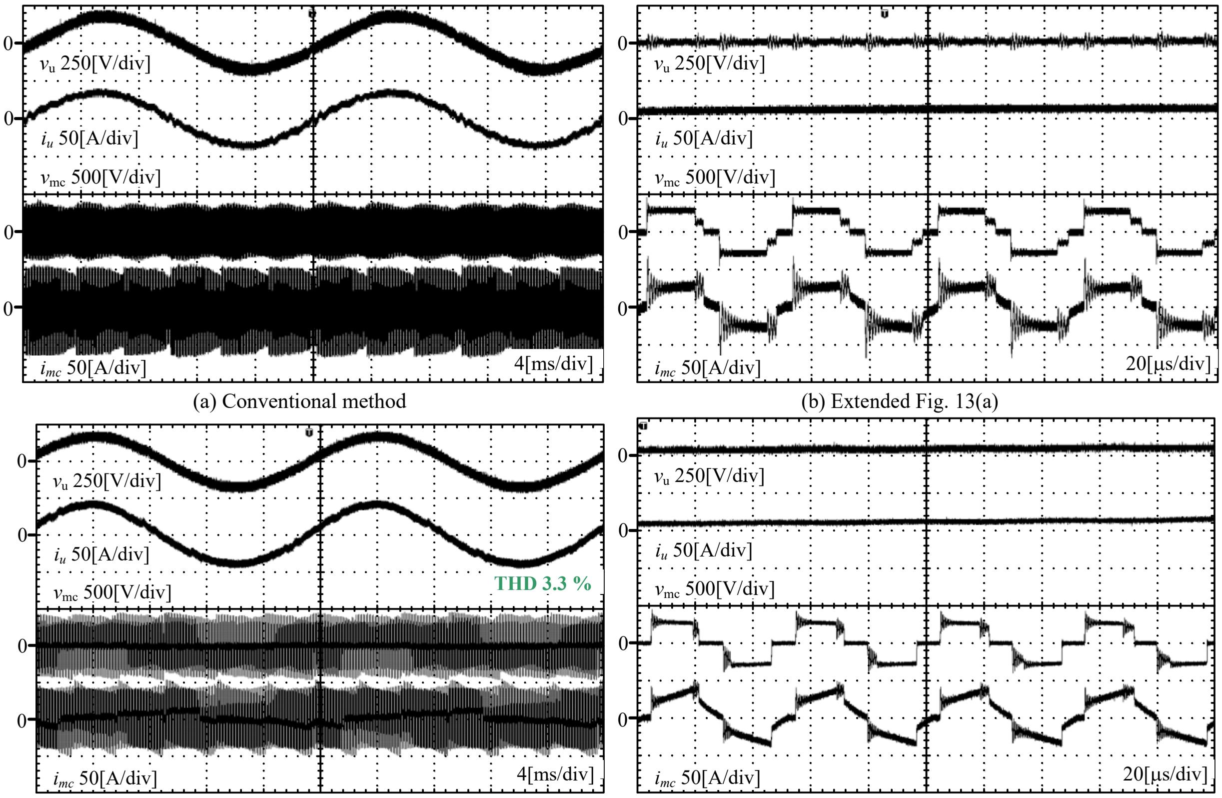

(a) Conventional method (b) Extended Fig. 13(a)

(c) Proposed method (d) Extended Fig. 13(c)

Fig. 13. Input and output waveforms of matrix converter at rated power of 10 kW. The DC voltage is 400 V.

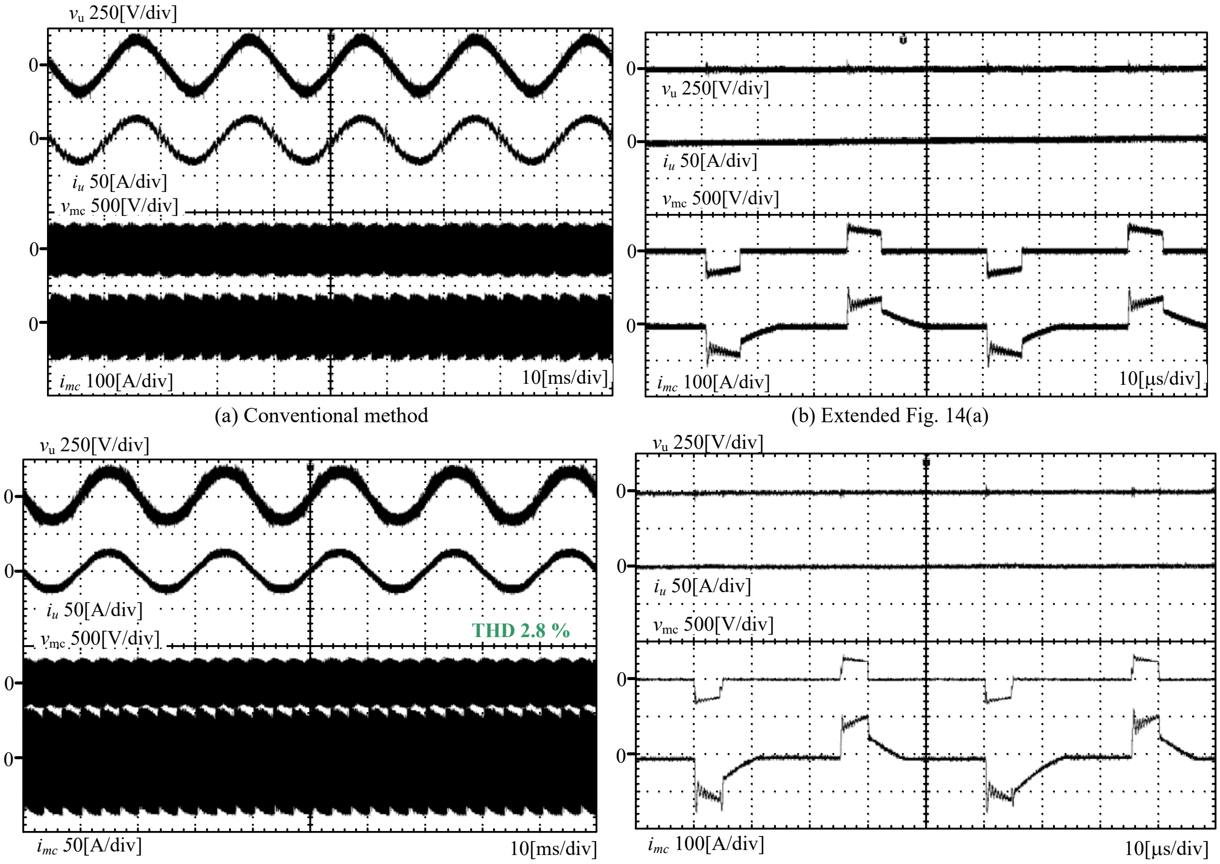

(a) Conventional method (b) Extended Fig. 14(a)

(c) Proposed method (d) Extended Fig. 14(c)

Fig. 14. Input and output waveforms of matrix converter at rated power of 0.6p.u.. The DC voltage is 200 V.

Figure 14 (a) and (b) show the experimental waveforms with the conventional method at the low modulation index. The dead-time-induced output voltage error occurs because the duty is shorter than the dead-time. As a result, the input current THD becomes high at 8.1%. Meanwhile, Figure 14 (c) and (d) show the experimental waveforms with the

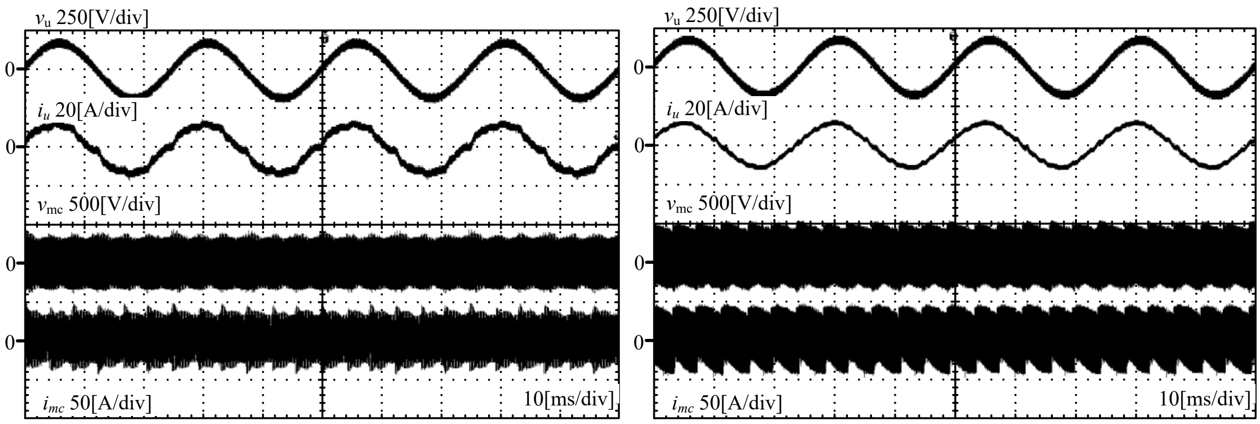

(a) Conventional method (b) Proposed method

Fig. 15. Input and output waveforms of matrix converter at 0.2p.u. of the rated power. The DC voltage is 400 V. The input current THD is greatly reduced from 8.2% to 5.3% by the proposed cancellation method.

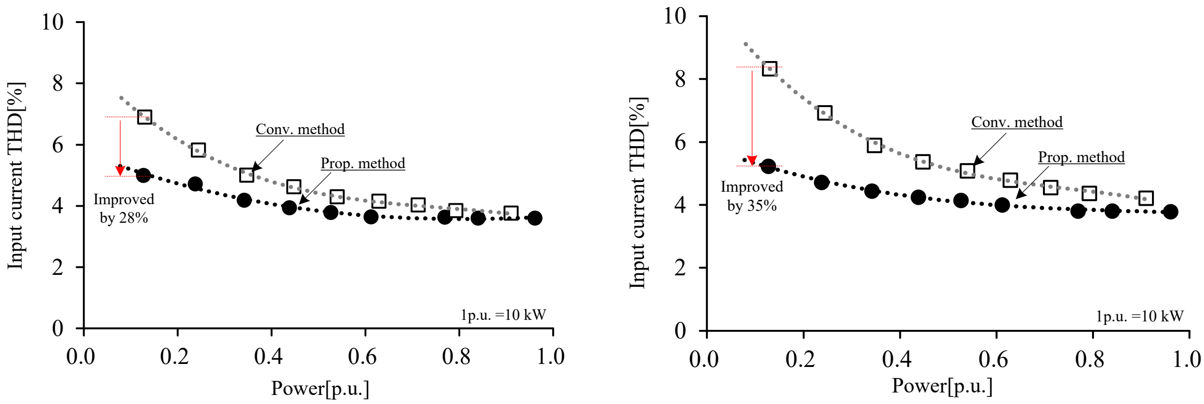

(a) Ripple current ratio is 10% (b) Ripple current ratio is 20%

Fig. 16. Relationship between input current THD and input power. The input current THD is improved by the proposed method regardless of the current ripple ratio.

proposed method at the low modulation index. The output voltage error does not occur thanks to the extension of the minimum duty. The low input current THD of 2.8% is achieved even with a low modulation index and low power of 0.6p.u..

Figure 15(a) and (b) show the input and output waveforms of matrix converter at 0.2p.u. of the rated power. The input current distortion is high at 8.2% with the conventional method due to the DC current ripple. The input current distortion is suppressed by the cancellation of the DC current ripple to apply the proposed method. As a result, the input current THD is improved by 35% compared with the conventional method.

Figure 16(a) and (b) show the input current THD characteristics with the current ripple ratio of 10% and 20% respectively. In the conventional method, the current ripple at the DC side is not ignored at the light load. Therefore, the input current is distorted due to the DC current ripple component with the traditional SVM. The input current distortion with the proposed method is improved from 8.2% to 5.3% by 35% compared with the conventional one.

Figure 17 shows the efficiency characteristics of the conventional and proposed method. The maximum efficiency is 91.7% with the proposed method. The efficiencies with the conventional and proposed method are almost the same. By applying the proposed method, the input current distortion is suppressed by the DC ripple cancellation to keep the high efficiency.

IV. Conclusion

In this paper, the dc current ripple cancelation was proposed to improve the input current THD. The proposed method eliminated the ripple component by the combination of the current slope during the positive and negative cycles of the high-frequency current. The amplitude of the DC current ripple was clarified to design the inductor at dc side with the proposed method. The 5^{th} and 7^{th} order harmonic components were decreased by over 95% with the proposed method in the simulation. As experimental results, the fundamental operations with the conventional method and proposed method were obtained. The input current THD is improved by 35% to cancel the DC current ripple at the light load.

In the future works, the improvement of the input current THD with a discontinuous current mode will be conducted.

REFERENCES

[1] Kyungmin Sung, Taisei Nishino, and Motohiro Takayasu"A Power-Assistance System using a Battery and an Electric Double-Layer Capacitor Bank for Light Electric Vehicles," IEEJ Journal of Industry Applications, vol. 8, no. 3, pp. 465-470, 2019.

[2] Fuka Ikeda, Toshihiko Tanaka, Hiroaki Yamada, and Masayuki Okamoto,"Constant DC-Capacitor Voltage-Control-Based Harmonics Compensation Algorithm of Smart Charger for Electric Vehicles in Single-Phase Three-Wire Distribution Feeders" IEEJ Journal of Industry Applications, vol.5, no.5, pp.405-406, 2016.

[3] S. Kim and F. Kang, "Multifunctional Onboard Battery Charger for Plug-in Electric Vehicles," in IEEE Transactions on Industrial Electronics, vol. 62, no. 6, pp. 3460-3472, June 2015.

[4] J. Everts, F. Krismer, J. Van den Keybus, J. Driesen and J. W. Kolar, "Comparative evaluation of soft-switching, bidirectional, isolated AC/DC converter topologies," 2012 Twenty-Seventh Annual IEEE Applied Power Electronics Conference and Exposition (APEC), Orlando, FL, 2012, pp. 1067-1074.

[5] L. Gu and K. Jin, "A Three-Phase Bidirectional AC/DC Converter With Y–Δ Connected Transformers," in IEEE Transactions on Power Electronics, vol. 31, no. 12, pp. 8115-8125, Dec. 2016.

[6] W. W. Chen, R. Zane and L. Corradini, "Isolated Bidirectional Grid-Tied Three-Phase AC–DC Power Conversion Using Series-Resonant Converter Modules and a Three-Phase Unfolder," in IEEE Transactions on Power Electronics, vol. 32, no. 12, pp. 9001-9012, Dec. 2017.

[7] B. Feng, H. Lin and X. Wang, "Modulation and control of ac/dc matrix converter for battery energy storage application," in IET Power Electronics, vol. 8, no. 9, pp. 1583-1594, 9 2015.

[8] B. Feng, H. Lin, X. Wang, X. An and B. Liu, "Optimal zero-vector configuration for space vector modulated AC-DC matrix converter," 2012 IEEE Energy Conversion Congress and Exposition (ECCE), Raleigh, NC, 2012, pp. 291-297.

[9] Inagaki et al., "A new PWM control method for AC to DC converters with high-frequency transformer isolation," Conference Record of the IEEE Industry Applications Society Annual Meeting,, San Diego, CA, USA, 1989, pp. 783-789.

[10] S. Ratanapanachote, Han Ju Cha and P. N. Enjeti, "A digitally controlled switch mode power supply based on matrix converter," in IEEE Transactions on Power Electronics, vol. 21, no. 1, pp. 124-130, Jan. 2006.

[11] V. Vlatkovic, D. Borojevic and F. C. Lee, "A zero-voltage switched, three-phase isolated PWM buck rectifier," in IEEE Transactions on Power Electronics, vol. 10, no. 2, pp. 148-157, March 1995.

[12] E. Joung, S. H. Huh, J. S. Kim, D. S. Hyun, J. Y. Choi and G. Choe, "A soft-switched DSP based isolated three-phase PWM buck rectifier," Proceedings of Power and Energy Systems in Converging Markets, Melbourne, Victoria, Australia, 1997, pp. 338-343.

[13] J. Afsharian, D. David Xu, B. Gong and Z. Yang, "Space vector demonstration and analysis of zero-voltage switching transitions in three-phase isolated PWM rectifier," 2015 IEEE Energy Conversion Congress and Exposition (ECCE), Montreal, QC, 2015, pp. 2477-2484.

[14] T. Zhao, X. Guo, J. Su and D. Xu, "Improved space vector modulation for matrix converter based isolated rectifiers," IECON 2014 - 40th Annual Conference of the IEEE Industrial Electronics Society, Dallas, TX, 2014, pp. 1532-1536

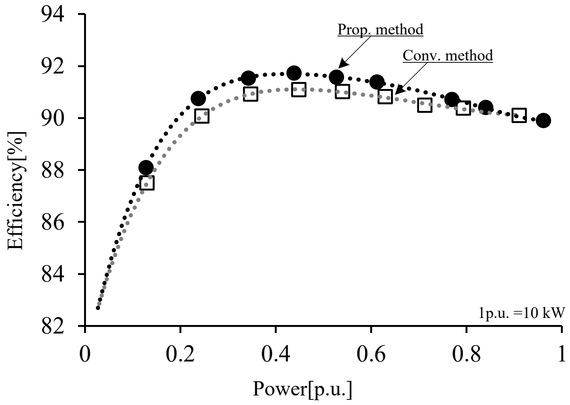

Fig. 17. Efficiency characteristics with conventional and proposed method.